A Loudness-based Adaptive, Higher-order Finite Element Method for Sonic Boom Propagation

R. Trono Figueras

David L. Darmofal, Marshall C. Galbraith, Steven R. Allmaras

MIT, Department of Aeronautics and Astronautics

Funded by NASA (#80NSSC22K0193)

April 11, 2025

Motivation For Sonic Boom Study

Ultimate goal:
Enable supersonic commercial flights overland.

Main challenge:

- Negative impact of sonic boom loudness on humans, other animals, and structures.

Study sonic boom to:

- Predict loudness sensitivities to airplane geometry.
- Perform airplane shape optimization to reduce loudness at ground.

Source: lockheedmartin.com

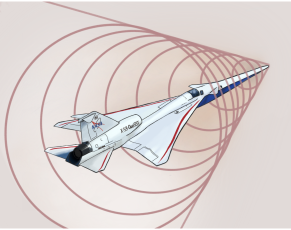

Source: michigandaily.com

Solution Approach: Broad Picture

Multidisciplinary design optimization[1]:

- Parametric geometry generator.
- CFD solver.
  - Euler/Navier-Stokes in 3D.
  - Uniform atmosphere.
- *Sonic boom propagation tool*
  - 2D problem.
  - Weakly non-linear.
  - Species relaxation.
  - Non-uniform atmosphere.
- Numerical optimizer.

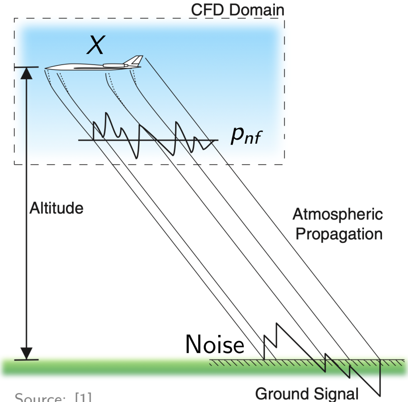

Source: [1]

Compute noise at ground and

$$\frac{d(\text{Noise})}{dX} = \boxed{\frac{\partial(\text{Noise})}{\partial p_{nf}}} \frac{dp_{nf}}{dX} .$$

[1] D. L. Rodriguez et. al. 2025

Propagation Problem: Motivation for Mesh Adaptation

Results for standard time-marching methods[2]:

Error in noise

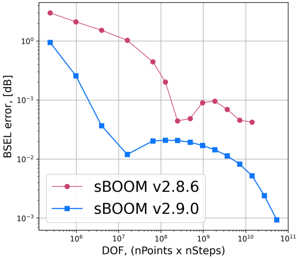

Source: [2]

($\approx 10^{11}$ DOF for 10^{-3} error)

Error in $|\partial(\text{Noise})/\partial p_{nf}|$

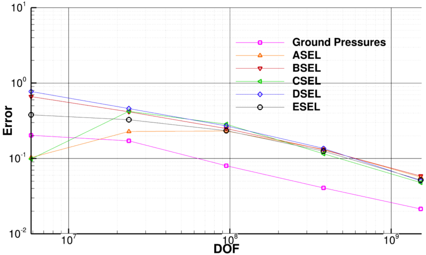

Source: [2]

($\approx 10^{10}$ DOF for 10^{-2} error)

Our goal: Reduce the significant computational cost involved. Enable efficient, automated high accuracy predictions of boom propagation and design sensitivities through adaptive control of numerical error.

[2] S. K. Rallabhandi et. al. 2023

Boom Propagation Modeling and Adaptive Approach

Coordinate System

Airplane at cruise altitude and cruise Mach number (M_a):

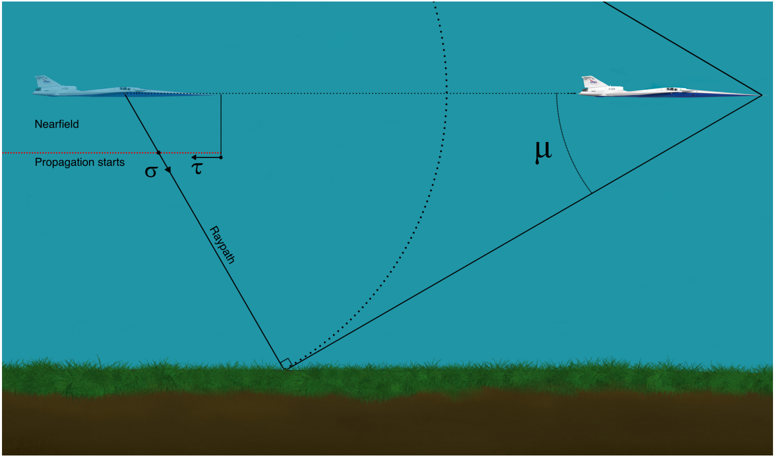

Mach cone angle: $\mu = \sin^{-1}(1/M_a)$.

Augmented Burgers System

To model sonic boom propagation we use the augmented Burgers system of equations, for the states $(P, \tilde{P}_{O_2}, \tilde{P}_{N_2})$:

$$\frac{\partial P}{\partial \sigma} - \frac{1}{2}\frac{\partial \ln(\rho_0 c_0 / A_{n0})}{\partial \sigma} P - \frac{1}{2}\frac{\partial P^2}{\partial \tau} - \frac{1}{\Gamma}\frac{\partial^2 P}{\partial \tau^2} - \frac{\partial}{\partial \tau}\left(\sum_{\nu} C_\nu \frac{\partial \tilde{P}_\nu}{\partial \tau}\right) = 0 \text{ on } \Omega, \quad (1)$$

$$-\frac{\partial \tilde{P}_\nu}{\partial \tau} + \frac{P - \tilde{P}_\nu}{\theta_\nu} = 0 \text{ on } \Omega, \qquad \nu = \{O_2, N_2\}, \quad (2)$$

which includes:

- Thermoviscous diffusion.
- Atmospheric absorption by relaxation species (O_2 and N_2).
- Ray tube area variation.

Remarks:

- Eq (1) is parabolic, with σ the time-like direction.
- It is typically solved with a time-marching scheme.

Atmosphere Model: Standard

Atmosphere model refers to how the atmospheric properties depend on altitude.

Standard model: First two layers:

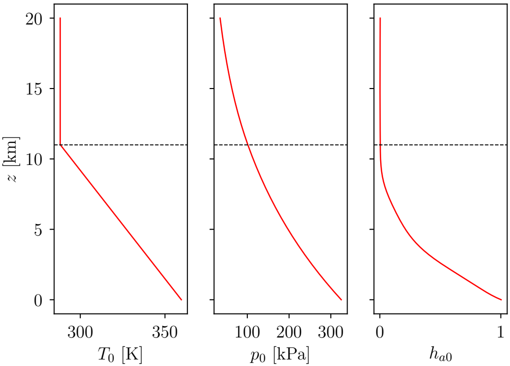

Additionally, models for:

- Density and speed of sound: ρ_0, c_0,
- Gol'berg number: Γ,
- Relaxation coefficients: C_ν, θ_ν,
- Ray tube area: A_{n0},

as functions of atmospheric properties.

Space-time Adaptive Method

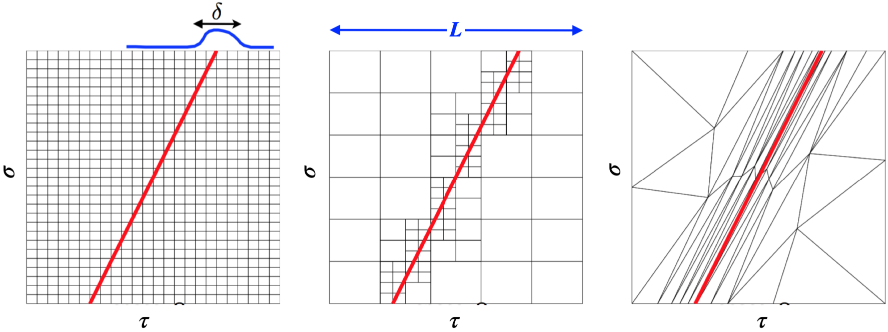

(a) uniform $\text{DOF} = O\left((L/\delta)^2\right)$

(b) space-time tensor-product $\text{DOF} = O\left(L/\delta\right)$

(c) space-time unstructured $\text{DOF} = O\left(1\right)$

But, space-time unstructured requires coupled solve over entire space-time domain.

Output-based Adaptation Cycle

Output of interest: Loudness at ground.

Adaptive cycle scheme:

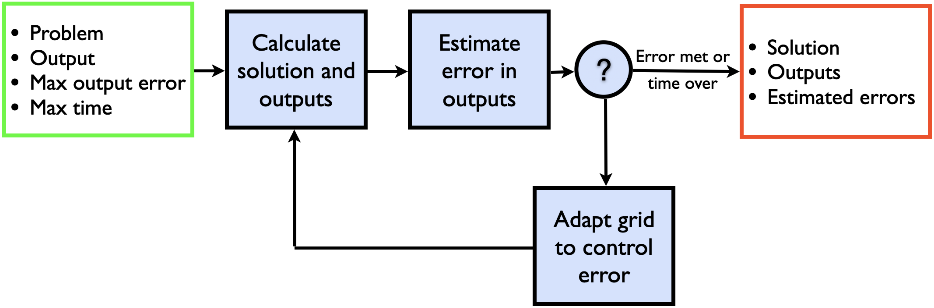

Discretization and Shock Capturing

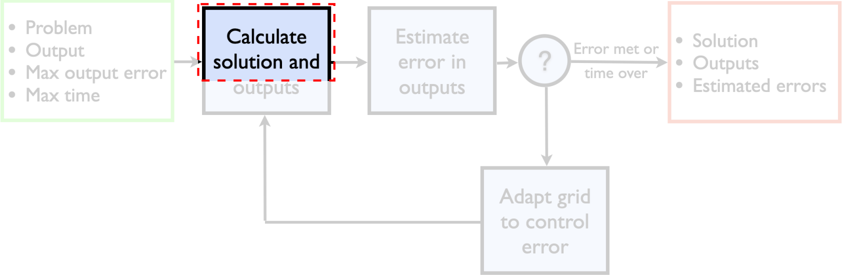

Continuous Galerkin type FEM

CG weak statement:

Find $\boldsymbol{u}_h \in \mathcal{V}_{h,p}$ such that:

$$\mathcal{R}(\boldsymbol{v}_h, \boldsymbol{u}_h) = 0, \quad \forall \boldsymbol{v}_h \in \mathcal{V}_{h,p}, \tag{3}$$

where the space $\mathcal{V}_{h,p}$ contains polynomials of order p in Ω.

Remarks:

- A discontinuous subscale is used for stabilization, and the resulting method is known as Variational Multiscale with Discontinuous Subscales.
- The discretization is adjoint consistent.

The Need for Artificial Viscosity

Challenge: Discontinuities (shocks) in the solutions, leading to unstable numerical solves and lack of convergence.

Goal: Smoothen discontinuities to improve stability, while not modifying the already smooth areas.

Approach: Employ a shock sensor, s, to keep track of discontinuities, and use that information to add localized artificial viscosity.

Add extra diffusion term in Burgers equation:

$$\frac{\partial P}{\partial \sigma} - \frac{1}{2}\frac{\partial \ln(\rho_0 c_0 / A_{n0})}{\partial \sigma} P - \frac{1}{2}\frac{\partial P^2}{\partial \tau} - \frac{1}{\Gamma}\frac{\partial^2 P}{\partial \tau^2} - \frac{\partial}{\partial \tau}\left(\sum_{\nu} C_\nu \frac{\partial \tilde{P}_\nu}{\partial \tau}\right) \underbrace{- \frac{\partial}{\partial \tau}\left(\epsilon_{\mathrm{AV}} \frac{\partial P}{\partial \tau}\right)}_{\text{extra term}} = 0, \quad (4)$$

with ϵ_{AV} as:

$$\epsilon_{\mathrm{AV}} := \underbrace{\frac{1}{2}\frac{H_{\tau\tau}}{p}|P|}_{\mathrm{AV}_{\max}} s. \quad (5)$$

PDE-based Shock Sensor[3]

Shock sensor design requirements:

- $s \approx 1$ in shock areas, of order $\mathcal{O}(h)$.
- $s \approx 0$ away from shocks, of order $\mathcal{O}(h^p)$.
- s smooth.

Define PDE for shock sensor s:

$$\underbrace{s - C_1 s_{\text{grad}}}_{\text{source term}} + \underbrace{C_2 \nabla \cdot \left(\frac{H^T H}{p^2} \nabla s \right)}_{\text{diffusion term}} = 0 \text{ on } \Omega. \tag{6}$$

- s_{grad}: **Shock indicator** based on pressure solution gradient.
- Diffusion term: to have a smooth sensor solution.
- H: element size field.

[2] G. E. Barter and D. L. Darmofal 2007

Shock Indicator s_{grad}

Starting point:

$$\xi := \frac{H_{\tau\tau}}{p}\left|\frac{\partial P}{\partial \tau}\right|, \quad \hat{\xi} = \frac{\xi}{\xi_1}, \tag{7}$$

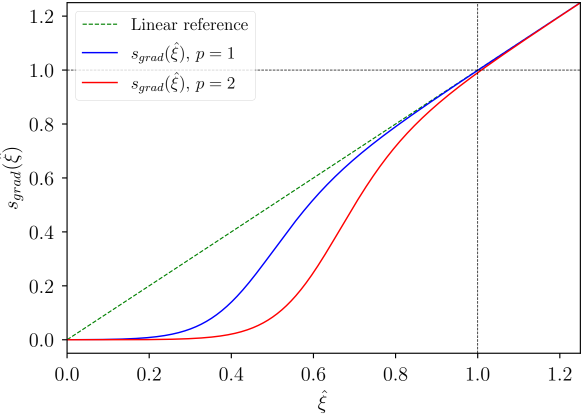

Test With Smooth Problem

Smooth problem with available exact solution:

- Solve without artificial viscosity.
- Solve with artificial viscosity and see how it affects convergence.

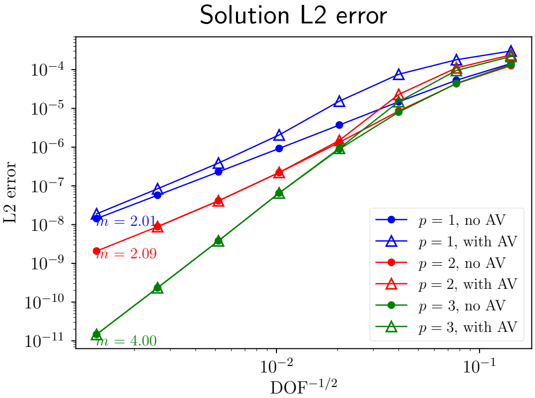

Test With Smooth Problem

Smooth problem with available exact solution:

- Solve without artificial viscosity.
- Solve with artificial viscosity and see how it affects convergence.

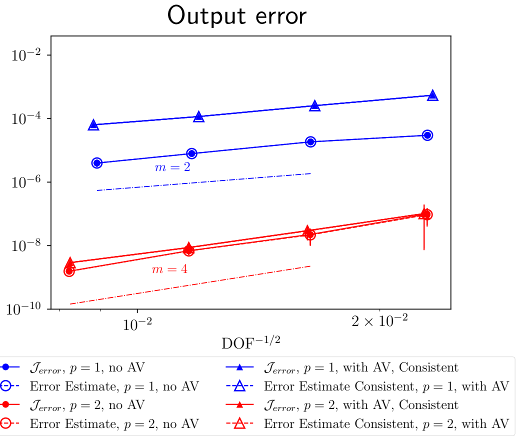

Ground Signal Filtering

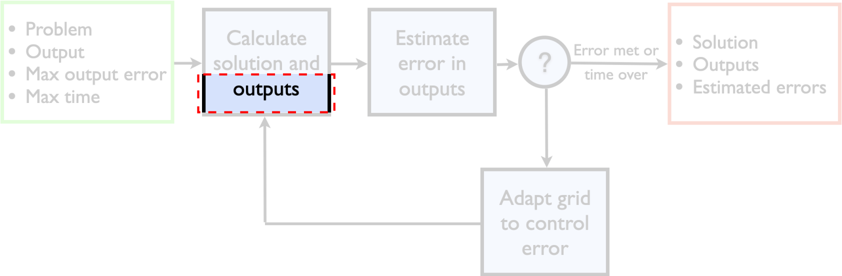

Relevant Loudness Metrics

The human ear is less sensitive to low audio frequencies.

There is a family of weighting filter curves that account for this relative loudness perceived by humans: A/B/C/D/-SEL curves.

$$\underbrace{p(\tau)}_{\text{Ground pressure signal}} \quad \rightarrow \quad \text{Weighting filter} \quad \rightarrow \quad \underbrace{\tilde{p}(\tau)}_{\text{Filtered signal}}$$

Sound exposure:

$$E = \frac{1}{\omega_{\text{ref}}} \int_{\tau_0}^{\tau_f} [\tilde{p}(\tau)]^2 \, d\tau. \tag{8}$$

Loudness level in dB:

$$\text{Loudness} = 10 \log_{10} \left(\frac{E}{E_0} \right), \quad E_0 = 400 \; (\mu\text{Pa})^2 s. \tag{9}$$

B-SEL Metric

We focus on the B-SEL curve, and the approach can be generalized to any other.

Transfer function in the complex frequency domain:

$$H_B(s) = \frac{\tilde{P}(s)}{P(s)} = \frac{c_B s^3}{(s + 2\pi f_1)^2 (s + 2\pi f_{2B})(s + 2\pi f_4)^2}, \quad (10)$$

- $c_B = 5.99185 \times 10^9$
- $f_1 = 20.598997$ Hz
- $f_{2B} = 158.48932$ Hz
- $f_4 = 12194.217$ Hz

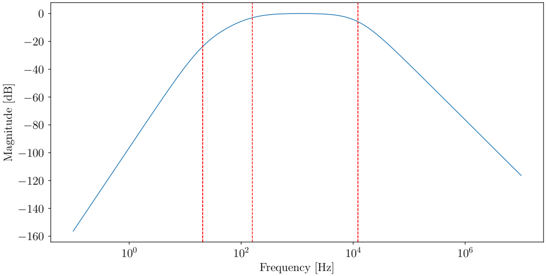

Filter Application: ODE Approach

Common filtering techniques not suitable for our unstructured grid.

Convert transfer function in complex frequency domain:

$$\tilde{P}(s) = P(s)\frac{K^{1/3}}{(s+a)^2}\frac{K^{1/3}s^2}{(s+c)^2}\frac{K^{1/3}s}{(s+b)}, \tag{11}$$

to a **system of ODE's** in the time domain (to solve in *ground* boundary):

$$\frac{d\bar{u}}{d\tau} = \begin{pmatrix} 0 & 1 & 0 & 0 & 0 \\ -a^2 & -2a & 0 & 0 & 0 \\ 0 & 0 & 0 & 1 & 0 \\ -K^{1/3}a^2 & -2K^{1/3}a & -c^2 & -2c & 0 \\ 0 & 0 & 0 & K^{1/3} & -b \end{pmatrix} \bar{u} + \begin{pmatrix} 0 \\ K^{1/3}p(\tau) \\ 0 \\ K^{2/3}p(\tau) \\ 0 \end{pmatrix}, \tag{12}$$

where $\bar{u} = (u_0, u_1, u_2, u_3, \tilde{p})^T$, with homogeneous initial conditions.

Output Error Estimation

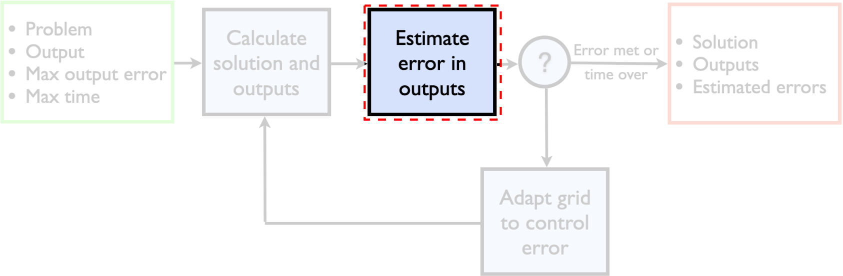

Output Functional

In general, consider output functional of the form:

$$\mathcal{J}(\boldsymbol{u}) := \int_{\Omega} g_v(\boldsymbol{u})dV + \int_{\partial\Omega} g_b(\boldsymbol{u})dS. \tag{13}$$

We define output error as:

$$\varepsilon(\boldsymbol{u}_h) := \mathcal{J}(\boldsymbol{u}) - \mathcal{J}(\boldsymbol{u}_h). \tag{14}$$

For general nonlinear problem, the output error can be approximated using the **dual weighted residual** (DWR) method.

Needs **correction**[4] for asymptotically consistent problems.

[4] B. Couchman 2020

Residual Consistency

- We say the residual form $\mathcal{R}$ is consistent if:

$$\mathcal{R}(\boldsymbol{v}_h, \boldsymbol{u}) = 0, \quad \forall \boldsymbol{v}_h \in \mathcal{V}_h, \tag{15}$$

  where $\boldsymbol{u}$ is the exact solution.
- We say the residual form $\mathcal{R}$ is asymptotically consistent if:

$$\mathcal{R}(\boldsymbol{v}_h, \boldsymbol{u}) = \mathcal{O}(h^\alpha), \quad \forall \boldsymbol{v}_h \in \mathcal{V}_h, \tag{16}$$

  where $\boldsymbol{u}$ is the exact solution, $\alpha > 0$, and h is a characteristic element size in $\mathcal{T}_h$.

In our situation:

$$\mathcal{R}(\boldsymbol{v}_h,\boldsymbol{u}_h) = \mathcal{R}^C(\boldsymbol{v}_h, \boldsymbol{u}_h) + \underbrace{\mathcal{R}^A(\boldsymbol{v}_h, \boldsymbol{u}_h)}_{\text{AV term}}. \tag{17}$$

Dual Problem and Error for Linear Case

We assume linear residual and output functional, and define the **dual** (adjoint) problem as:

Find $\psi \in \mathcal{W}$ such that:

$$\mathcal{R}(\psi, \boldsymbol{w}) - \mathcal{J}(\boldsymbol{w}) = 0, \quad \forall \boldsymbol{w} \in \mathcal{W}. \tag{18}$$

From there:

$$\begin{aligned}
\varepsilon(\boldsymbol{u}_h) &= \mathcal{J}(\boldsymbol{u}) - \mathcal{J}(\boldsymbol{u}_h) \\
&= \mathcal{J}(\Delta \boldsymbol{u}) \\
&= \mathcal{R}(\psi, \Delta \boldsymbol{u}) \\
&= \underbrace{\mathcal{R}^C(\psi, \boldsymbol{u})}_{=0} + \mathcal{R}^A(\psi, \boldsymbol{u}) \underbrace{- \mathcal{R}^C(\psi, \boldsymbol{u}_h) - \mathcal{R}^A(\psi, \boldsymbol{u}_h)}_{=-\mathcal{R}(\psi, \boldsymbol{u}_h)} \\
&= -\Big[\mathcal{R}(\psi, \boldsymbol{u}_h) - \mathcal{R}^A(\psi, \boldsymbol{u})\Big] \text{ (Dual weighted residual error expression)}
\end{aligned} \tag{19}$$

Approximations: DWR Error Estimate

So far:

$$\varepsilon(\boldsymbol{u}_h) = -\Big[\mathcal{R}(\psi, \boldsymbol{u}_h) - \mathcal{R}^A(\psi, \boldsymbol{u})\Big]. \tag{20}$$

Issues:

- Primal exact solution $\boldsymbol{u}$ is not available.
- Residual and output functional are in general nonlinear.
- Even if they are linear, adjoint exact solution ψ is not available.

First approximation:

$$\mathcal{R}^A(\psi, \boldsymbol{u}) \approx \mathcal{R}^A(\psi, \boldsymbol{u}_h), \tag{21}$$

justified on a shock dominated problem with AV.

Approximations: DWR Error Estimate

Second approximation:

ψ is approximated with a numerical adjoint $\psi_{\hat{h}}$ defined by[5]:
$\psi_{\hat{h}} \in \mathcal{V}_{\hat{h},\hat{p}}$ such that:

$$\mathcal{R}'[\boldsymbol{u}_h](\psi_{\hat{h}}, \tilde{\boldsymbol{u}}) - \mathcal{J}'[\boldsymbol{u}_h](\tilde{\boldsymbol{u}}) = 0, \quad \forall \tilde{\boldsymbol{u}} \in \mathcal{V}_{\hat{h},\hat{p}}, \tag{22}$$

where:

- $\mathcal{R}'[\boldsymbol{u}_h]$ and $\mathcal{J}'[\boldsymbol{u}_h]$ are the linearizations of $\mathcal{R}$ and $\mathcal{J}$ about $\boldsymbol{u}_h$.
- $\tilde{\boldsymbol{u}}$ represents a perturbation from $\boldsymbol{u}_h$.
- The space $\mathcal{V}_{\hat{h},\hat{p}}$ contains polynomials of order $\hat{p} = p + 1$.

Final DWR error estimate:

$$\varepsilon(\boldsymbol{u}_h) \approx -\Big[\mathcal{R}(\psi_{\hat{h}}, \boldsymbol{u}_h) - \mathcal{R}^A(\psi_{\hat{h}}, \boldsymbol{u}_h)\Big]. \tag{23}$$

[5] M. Yano and D. L. Darmofal 2012

Mesh Adaptation

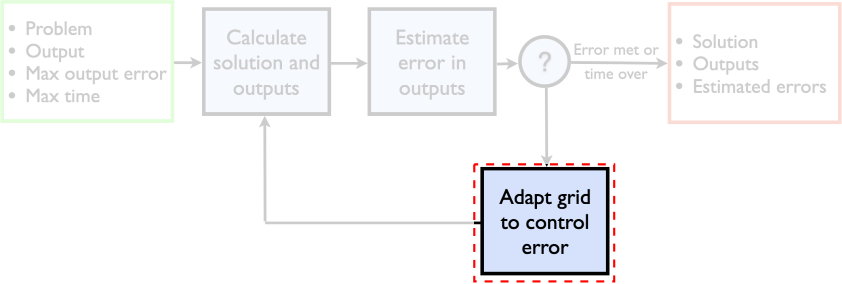

Continuous Optimization: Mesh-Metric Duality

Want mesh producing the smallest output error indicator $\mathcal{E}$:

$$\hat{\mathcal{T}}_h = \arg \inf_{\mathcal{T}_h \in \mathbb{T}(\Omega)} \mathcal{E}(\mathcal{T}_h), \quad \mathcal{C}(\mathcal{T}_h) < C. \tag{24}$$

Continuous relaxation[6] to address intractability of discrete problem.

$$\hat{\mathcal{M}} = \arg \inf_{\mathcal{M} \in \mathbb{M}(\Omega)} \mathcal{E}(\mathcal{M}), \quad \mathcal{C}(\mathcal{M}) < C \tag{25}$$

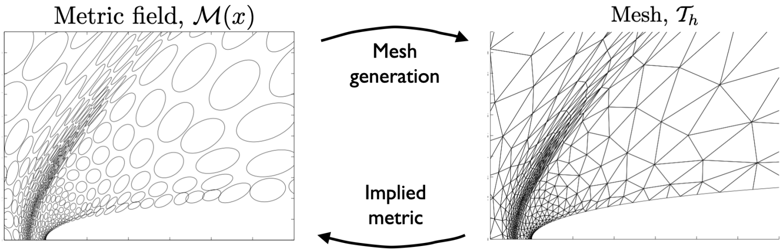

[6] A. Loseille and F. Alauzet 2011

MOESS[8]: Error Sampling and Synthesis

Need model for error indicator $\mathcal{E}(\mathcal{M})$: How $\mathcal{E}$ changes with $\mathcal{M}$.

First step: Compute nodal[7] error indicators based on the DWR error estimate. Use partition of unity given by linear tent functions $\{\phi_v\}$.

$$\varepsilon_v = -\mathcal{R}(\phi_v \psi_{\hat{h}}, \boldsymbol{u}_h) + \mathcal{R}^A(\phi_v \psi_{\hat{h}}, \boldsymbol{u}_h), \tag{26}$$

$$\eta_v := |\mathcal{R}(\phi_v \psi_{\hat{h}}, \boldsymbol{u}_h)| + |\mathcal{R}^A(\phi_v \psi_{\hat{h}}, \boldsymbol{u}_h)|, \quad \eta := \sum_v \eta_v \equiv \mathcal{E} \tag{27}$$

Next: Recompute solution and nodal indicators in refined *local patches* in the mesh.

The comparison of the nodal error indicators before and after the local solves gives information about how $\mathcal{E}$ changes with $\mathcal{M}$.

[7] T. Richter and T. Wick 2015

[8] M. Yano and D. L. Darmofal 2012

MOESS: Error Sampling and Synthesis

Local solves: Loop over edges in the mesh and solve for $\boldsymbol{u}_h^\epsilon$ in refined local patch. $\mathcal{R}_{\text{local}}(\boldsymbol{v}_h^\epsilon, \boldsymbol{u}_h^\epsilon) = 0, \quad \forall \boldsymbol{v}_h^\epsilon \in \mathcal{V}_{h,p}^\epsilon$.

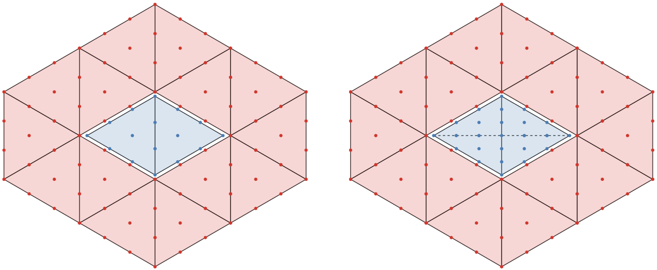

(a) Unsplit **(b)** Split

Nodal indicator for vertices in inner patch:

$$\eta_v^\epsilon = |\mathcal{R}_{\text{local}}(\phi_v \psi_{\hat{h}}, \boldsymbol{u}_h^\epsilon)| + |\mathcal{R}_{\text{local}}^A(\phi_v \psi_{\hat{h}}, \boldsymbol{u}_h^\epsilon)|. \tag{28}$$

Results for Practical Case

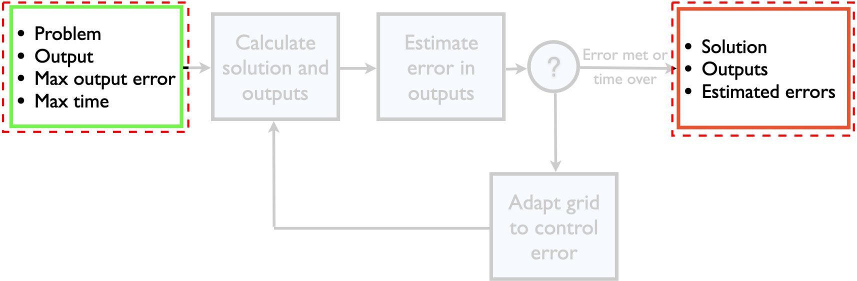

Preliminary: Implementation Notes

Software: Solution Adaptive Numerical Simulator (SANS)[9]

- C++ framework to numerically solve partial differential equations.
- Extensive use of templates for efficient yet general code.
- Supports several CG and DG discretizations, with output-based mesh adaptation.
- Automatic differentiation via operator overloading.
- MPI parallelization.
- Unit testing and continuous integration.
- Open source.

[9] Galbraith et. al. 2015

Preliminary: Run Summary

1. **Set:**
    - Case parameters/conditions.
    - Initial 2D mesh.
    - Target DOF.
    - Number of adaptive iterations (N).
2. **Loop,** $i \in \{1, ..., N\}$**:**
    - Extract *ground* boundary and form 1D mesh for filter ODE.
    - Solve primal problem:
        - [Burgers system + shock sensor] in 2D mesh.
        - Filter ODE in 1D mesh (ground boundary).
    - Solve adjoint problem:
        - Adjoint ODE in 1D mesh (ground boundary).
        - [Burgers system + shock sensor] adjoint in 2D mesh.
    - Nodal error sampling and synthesis.
    - Adapt mesh.

Case Description

- Airplane Mach number: $M_a = 1.4$.
- Airplane altitude: $z_a = 16459.2$ m.
- Ground altitude: 110 m.
- Ground reflection factor: 1.9.
- Nearfield signal (initial condition):

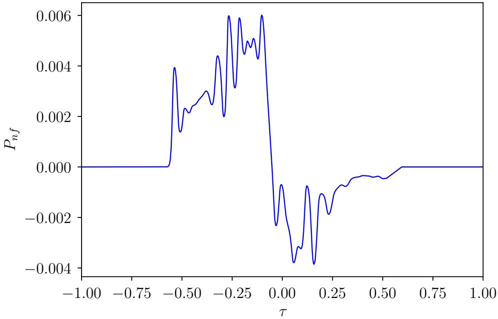

Source: lockheedmartin.com

- Domain dimensions: $\Omega = [-1, 2] \times [0, 257]$
- Output for adaptation: $\mathcal{J}_{\mathrm{BSEL}} = \int_{\mathrm{ground}} [\tilde{p}(t)]^2 \, dt$
- Also for comparison: $\mathcal{J}_p = \int_{\mathrm{ground}} [p(t)]^2 \, dt$

Propagation: Pressure Solution

$p = 1$

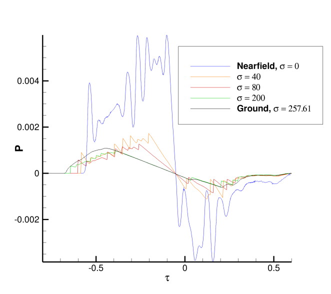

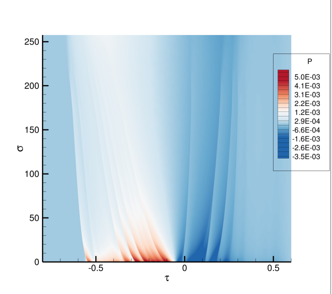

$p = 2$

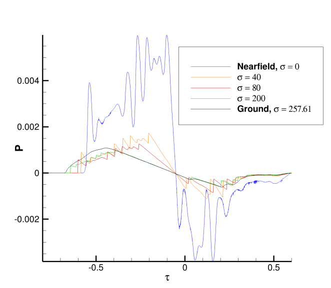

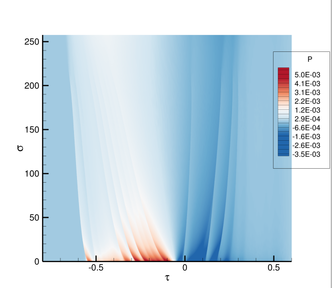

Propagation: Final Adapted Mesh for 8K Target DOF

$p = 1$

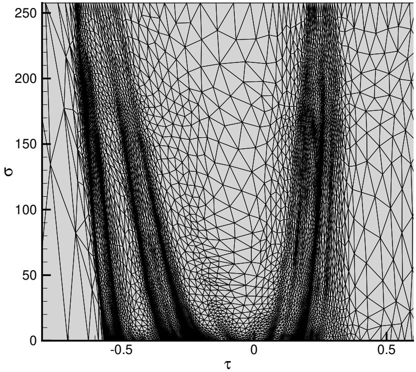

$p = 2$

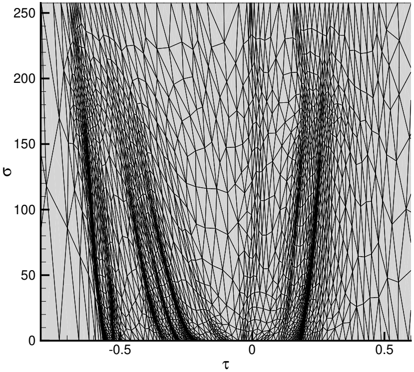

Propagation: Evolution Over Adaptive Cycle, 8K Target DOF

Different Adaptation Outputs and Their Adjoints

$\mathcal{J}_{\mathrm{BSEL}}$

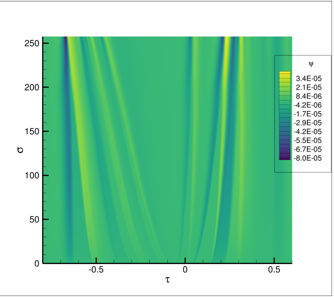

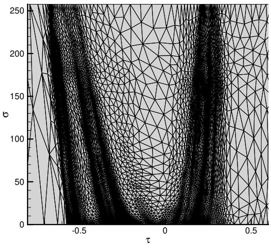

$\mathcal{J}_p$

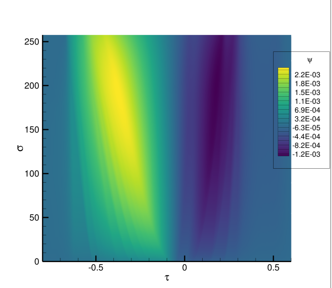

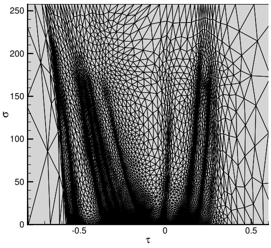

At Ground: Pressure Signal and Its Filtering

Pressure Signal

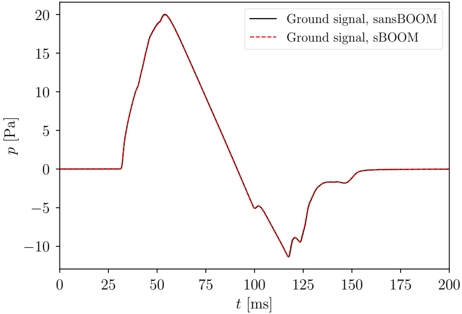

B-SEL Filter Output

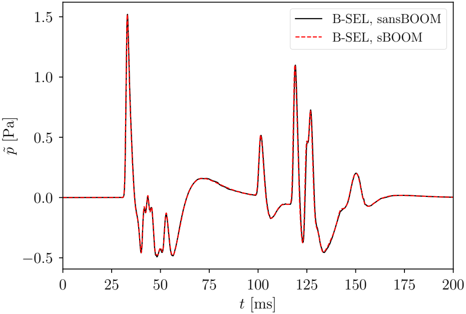

Comparison with NASA *sBOOM* code[10]:

- sansBOOM: 128K DOF in total (space-time).
- sBOOM:
  - 32K DOF in τ direction.
  - 39K steps (marching) in σ direction.
  - 1.2B DOF in total (space-time).

[10] S. K. Rallabhandi et. al. 2023

At Ground: Loudness Convergence with Mesh Refinement

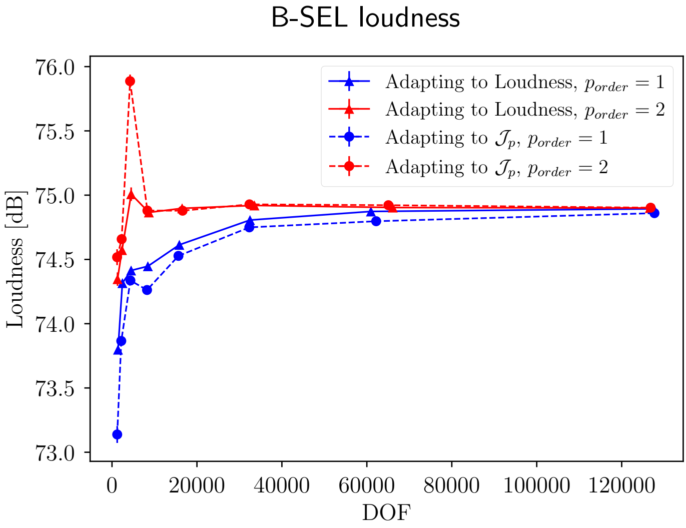

At Nearfield: Loudness Sensitivity

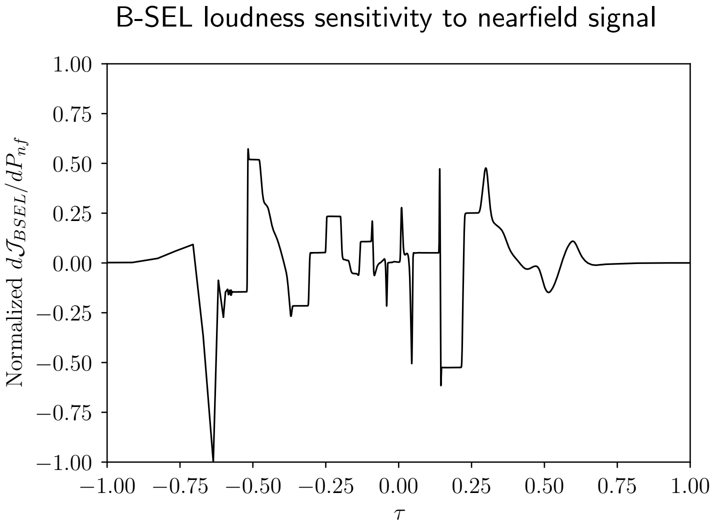

Concluding Remarks

Work completed:

- Higher-order FEM to solve sonic boom propagation problem.
- Unstructured space-time mesh adaptation.
- Loudness error estimate driving mesh adaptation.

Outcome:

- Significant reduction in space-time DOF count, at the expense of solving the dual problem.
- The above is highlighted when using higher-order solutions, as quadratic solutions converge the output faster than linear solutions.

Ongoing effort:

- Study convergence of loudness sensitivity to nearfield signal.

Thanks for the attention!

Questions?

Variational Multiscale with Discontinuous Subscales (VMSD) Method

Discretization of Ω:

$\mathcal{T}_h := \{\kappa\}_{\kappa=1}^{K}$ is a triangulation of the domain Ω into K elements.

Propose solution:

$\boldsymbol{u}_h := \bar{\boldsymbol{u}}_{h,p} + \boldsymbol{u}'_{h,p'}, \qquad \bar{\boldsymbol{u}}_{h,p} \in \overline{\mathcal{V}}_{h,p}, \quad \boldsymbol{u}'_{h,p'} \in \mathcal{V}'_{h,p'}.$

VMSD solution spaces:

$$(\textit{Coarse}\ \text{scale})\ \overline{\mathcal{V}}_{h,p} := \{\boldsymbol{v} \in [C^0(\Omega)]^m : \boldsymbol{v}|_\kappa \in [\mathcal{P}^p(\kappa)]^m, \forall \kappa \in \mathcal{T}_h\}, \quad (29)$$

$$(\textit{Fine}\ \text{scale})\ \mathcal{V}'_{h,p'} := \{\boldsymbol{v} \in [L^2(\Omega)]^m : \boldsymbol{v}|_\kappa \in [\mathcal{P}^{p'}(\kappa)]^m, \forall \kappa \in \mathcal{T}_h\}. \quad (30)$$

Variational Multiscale with Discontinuous Subscales (VMSD) Method

Weak statement:

Find $(\bar{\boldsymbol{u}}_{h,p}, \boldsymbol{u}'_{h,p'}) \in \overline{\mathcal{V}}_{h,p} \times \mathcal{V}'_{h,p'}$ **such that:**

$$\mathcal{R}(\bar{\boldsymbol{v}}_{h,p}, \boldsymbol{v}'_{h,p'}; \bar{\boldsymbol{u}}_{h,p}, \boldsymbol{u}'_{h,p'}) = 0, \quad \forall(\bar{\boldsymbol{v}}_{h,p}, \boldsymbol{v}'_{h,p'}) \in \overline{\mathcal{V}}_{h,p} \times \mathcal{V}'_{h,p'}. \tag{31}$$

Remarks:

- $\boldsymbol{u}'_{h,p'}$ DOFs are element-wise decoupled. Thus, they can be static condensed and the total cost becomes the same as a CG method.
- For same accuracy requirement, more efficient (less DOFs) than CG and DG.
- Adjoint consistent.

Shock Indicator s_{grad}

Starting point:

$$\xi := \frac{H_{\tau\tau}}{p}\left|\frac{\partial P}{\partial \tau}\right|, \quad \xi_1 \simeq \max_{x\in\Omega} \xi(x), \quad \hat{\xi} = \frac{\xi}{\xi_1}, \tag{32}$$

then:

$$s_{\text{grad}} := s_{\text{grad}}(\hat{\xi}) = \frac{\hat{\xi}[\tanh(p^2\hat{\xi})]^{p-1}}{1+\exp\left[-k\left(\hat{\xi}-\alpha(p)\right)\right]}, \tag{33}$$

where $k, \alpha(p) \in \mathbb{R}$.

Shock Indicator s_{grad}

$$s_{\text{grad}} := s_{\text{grad}}(\hat{\xi}) = \frac{\hat{\xi}[\tanh(p^2\hat{\xi})]^{p-1}}{1 + \exp\left[-k\left(\hat{\xi} - \alpha(p)\right)\right]}, \tag{34}$$